

- (1984). (22) A. E. Asku and D. J. W. Piper, *Mar. Geol.* **54**, 1 (1984). (23) reference (6). (24) L. I. Bogolyubova, *Lithol. Miner. Resour.* **25**, 54 (1990). (25) Y. F. Belevich, *Izv. Akad. Nauk SSSR Ser. Geograf.* **1987**, 82 (1987). (26a) P. Kassler, in *The Persian Gulf*, B. H. Purser, Ed. (Springer, New York, 1973), pp. 11–32; (26b) P. Sanlaville, *Paléorient* **15**, 5 (1989). (27) M. Umitsu, *Sediment. Geol.* **83**, 177 (1993). (28) J. R. P. Somboon and N. Thiramongkol, *J. S. E. Asian Earth Sci.* **7**, 53 (1992). (29) G. P. Allen, D. Laurier, J. P. Thouvenin, *TOTAL, Cie. Fr. Pet., Notes Mém.* **15**, 1 (1979). (30) Y. Zong, *J. Coastal Res.* **8**, 1 (1992). (31a) K.-B. Liu, S. Sun, X. Jiang, *Quat. Res.* **38**, 32 (1992); (31b) reference (14). (32) S. Mori, *J. Earth Sci. Nagoya Univ.* **34**, 109 (1986). (33) J. Chappell, *Sediment. Geol.* **83**, 339 (1993). (34) *ibid.*, p. 339; (35) B. G. Jones, G. R. Martin, N. Senapati, *ibid.*, p. 319. (36) P. S. Roy and E. A. Crawford, *Rec. Geol. Surv. N.S.W.* **20**, 160 (1981).
12. MEDIBA (Mediterranean Basin Program), *Nile Delta Project Database Listings*, (U.S. National Museum of Natural History Records, Washington, DC, 1994).
  13. Analysis is based on more than 4000 petrographic samples from 87 long drill cores [positions shown in (7)]. Almost all cores have been radiocarbon dated (total of ~400 dates), of which 64 dates were obtained from samples at or near the base of Holocene deltaic sequence III (Fig. 1).
  14. T. E. Törnqvist, *J. Sediment. Petrol.* **63**, 683 (1993); *Fluvial Sedimentary Geology and Chronology of the Holocene Rhine-Meuse Delta, The Netherlands* (Faculteit Ruimtelijke, Utrecht, The Netherlands, 1993).
  15. D. J. Stanley and Z. Chen, *Mar. Geol.* **112**, 1 (1993).
  16. P. C. Scruton, in *Recent Sediments, Northwest Gulf of Mexico*, F. P. Shepard, F. P. Phleger, T. J. H. van Andel, Eds. (American Association of Petroleum Geologists, Tulsa, OK, 1960), pp. 82–102.
  17. D. E. Frazier, *Tex. Bur. Econ. Geol. Geol. Circ.* **74-1** (1974).
  18. O. van de Plassche, Ed., *Sea-Level Research: A Manual for the Collection and Evaluation of Data* (Geo Books, Norwich, England, 1986); D. B. Scott, P. A. Pirazzoli, C. A. Honig, Eds., *Late Quaternary Sea-Level Correlation and Applications* (Kluwer Academic, Boston, 1989).
  19. R. G. Fairbanks, *Nature* **342**, 637 (1989).
  20. R. G. Lighty, I. G. Macintyre, R. Stuckenrath, *Coral Reefs* **1**, 125 (1982); W. S. Newman, R. R. Pardi,

- R. W. Fairbridge, in *Late Quaternary Sea-Level Correlation and Applications*, D. B. Scott, P. A. Pirazzoli, C. A. Honig, Eds. (Kluwer Academic, Boston, 1989), pp. 207–228.
21. N.-A. Mörner, in *Earth Rheology, Isotasy and Eustasy*, N.-A. Mörner, Ed. (Wiley, New York, 1980), pp. 535–553.
  22. A. G. Warne and D. J. Stanley, *Geology* **21**, 715 (1993).
  23. K. O. Emery and D. G. Aubrey, *Sea Levels, Land Levels and Tide Gauges* (Springer, New York, 1991).
  24. S. Postel, *Last Oasis: Facing Water Scarcity* (Norton, New York, 1992); International Bank for Reconstruction and Development–World Bank, *World Population Projections* (John Hopkins Univ. Press, Baltimore, 1993); C. Rosenzweig and M. L. Perry, *Nature* **367**, 133 (1994).
  25. We thank W. Autin, Z. Chen, I. G. Macintyre, W. A. DiMichele, R. T. Saucier, T. E. Törnqvist, J. Schneiderman, L. M. Smith, W. Pizzolato, M. K. Corcoran, and D. T. Steere Jr. for their assistance, advice, and reviews. Funding was provided by Smithsonian Scholarly Studies Program and National Geographic Society grants.

22 February 1994; accepted 13 May 1994

## “Molecule Corrals” for Studies of Monolayer Organic Films

David L. Patrick, Victor J. Cee, Thomas P. Beebe Jr.\*

Scanning tunneling microscopy (STM) studies have demonstrated that monolayer-deep, flat-bottomed, circular etch pits can be grown on highly ordered pyrolytic graphite by high-temperature etching in the presence of oxygen. In this work, these graphite etch pits are used as “molecule corrals” to isolate ensembles of molecules for study by STM. The nucleation of self-assembled molecular films in the corrals took place by nucleation events separate from those leading to self-assembly on the surrounding terrace and allowed the measurement of the nucleation rate constant in the corrals. The dependence of the nucleation rate for self-assembly on pit size shows that nucleation occurs at open terrace sites and that step edges (that is, the corral's perimeter) and confinement inhibit film growth.

Molecular self-assembly of organic thin films on solid surfaces has long been an area of interest in fields ranging from materials science to biology (1). Self-assembled films, in addition to exhibiting a rich variety of scientifically interesting properties, are promising candidates for use in a number of applications, from chemical sensors to nonlinear optical devices (2). In this report, we describe an investigation of self-assembled liquid crystal films on graphite designed to study (i) nucleation and growth processes in thin molecular films and (ii) the degree of interaction between molecules in adjacent molecular domains. A new approach, in which nanometer-sized “molecule corrals” are used to confine molecule ensembles within small regions, permits the analysis of molecular behavior by statistical methods and allows the measurement of several important properties difficult or impossible to

determine by other techniques. We show that etch pits offer a practical method for confining molecules to small surface regions and allow the observation of multiple independent sample domains with STM. Other researchers have built corrals atom by atom at 4 K to study the properties of confined wave functions (3); we use corrals to study the behavior of molecules on surfaces. The ease with which these corrals can be constructed using standard laboratory apparatus makes them appealing for use in a wide range of studies.

The construction of molecule corrals is based on a chemical modification of highly oriented pyrolytic graphite (HOPG) that occurs when it is heated in the presence of O<sub>2</sub> at ~650°C (4). Carbon removal by oxidation around preexisting point defects results in the creation of monolayer-deep, flat-bottomed etch pits with surface densities from 1 to 25 μm<sup>-2</sup> (5, 6). Circular etch pits with diameters between 50 and 5000 Å are readily formed, and their size can be accurately controlled by varying the heat-

ing temperature and time. Noncircular, irregularly shaped etch pits can also be made by repeated heating at 1000°C in air for short (~15 s) intervals.

The molecule used, 4'-octyl-4-biphenyl-carbonitrile (8CB), was chosen because many of its bulk and surface properties are known from previous studies (7), although preliminary experiments on other systems indicate that the use of molecule corrals is not limited to this molecule. We applied 8CB directly to etched HOPG surfaces as a neat liquid, in air at a slightly warm room temperature of 26° ± 1°C. At this temperature, 8CB is a bulk smectic-A phase with a thick, honey-like consistency. Each HOPG sample was covered with a macroscopic thickness of 8CB. The STM tip plunges through all intervening layers to image only the molecules directly adsorbed to the substrate (7).

The STM image in Fig. 1A shows three corrals, two of which are 800 Å in diameter and one that is 1400 Å in diameter, on an HOPG surface covered with a film of 8CB. The closely spaced (38 ± 1 Å) lines on the terrace and in two of the monolayer-deep corrals are parallel rows of self-assembled molecules adsorbed to the HOPG surface (8). The row structure in a low-resolution image like Fig. 1A arises from the molecular details of the unit cell, which are resolved in Fig. 1B, with an interrow spacing equal to βcos(90-θ), where β and θ are defined as in Fig. 1B. The image in Fig. 1A was taken several hours after the film was applied, and self-assembled monolayers had formed in two of the three corrals. The third corral, which appears empty, was likely filled with molecules in a disordered state [which cannot be imaged by STM because of the relative time scales of their thermal motion and image acquisition (9)].

Department of Chemistry, University of Utah, Salt Lake City, UT 84112, USA.

\*To whom correspondence should be addressed.

The image in Fig. 1A contains two points of interest. First, although there are correlations between the molecular structures in the corrals and those on the nearby terrace (discussed below), they are statistical in nature, suggesting that molecules in corrals order after events that occur separately from those on the terrace. Second,

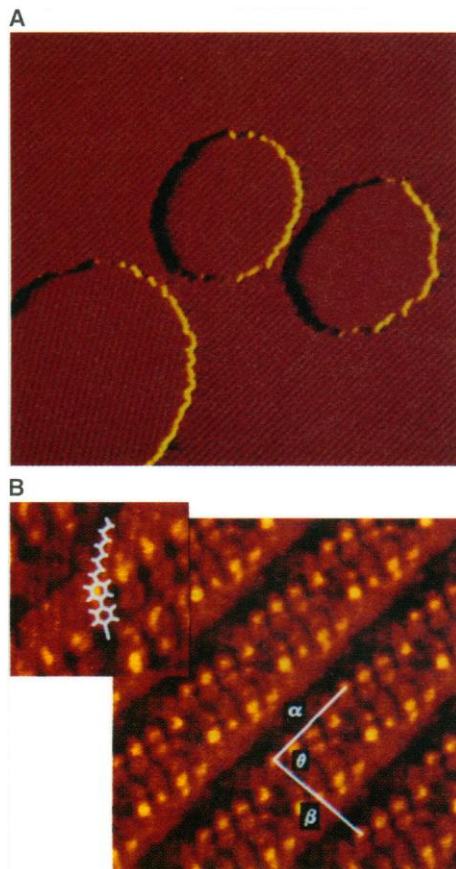


**Fig. 1.** Self-assembled molecular rows in corrals on graphite. **(A)** A 3000 Å by 3000 Å constant-height STM image of an ordered molecular monolayer of 8CB grown on an HOPG surface with corrals. The closely spaced lines are rows of molecules. The image was acquired several hours after the application of molecules to the surface, and ordered monolayer films had formed in two of the three corrals shown. Note that the molecular rows in one of the small corrals are aligned with those on the terrace whereas the rows in the large corral are not, and there is no ordering in the third corral. This and other images were obtained in constant-height mode, resulting in the apparent shading at the corral edges. All STM images are pixel-wise averages of five images, individually corrected for thermal drift. No additional image processing has been performed. **(B)** A 95 Å by 95 Å constant-height, molecular-resolution image of a representative 8CB structure on HOPG. The interrow spacing is 33 Å, with  $\alpha = 33^\circ$ ,  $\beta = 35^\circ$ , and  $\theta = 72^\circ$ . The inset shows a portion of a unit cell with the position of one molecule marked by a model overlay. The alkyl tails and the rings of the biphenyl moiety are simultaneously visible.

ordered films nucleate in corrals over a period of hours, and at any given time there may be a distribution of corrals filled with ordered and disordered molecules (10).

Evidence that nucleation for the ordering of molecules in corrals is initiated independently of ordering on the terrace is shown in Fig. 2. The image shows two corrals, one formed by chance inside another

(a very rare occurrence, dependent on the graphite crystal). Although the molecules in the first, outermost corral are in a disordered state, self-assembly has occurred in the inner corral on the lower level. Images such as Fig. 2 rule out the possibility that ordering in corrals is caused simply by propagation of ordering outside of them.

Because molecular self-assembly in each corral occurs by a distinct event, the rate of molecular ordering in corrals is well described by a first-order process with the integrated rate expression  $F_d = e^{-kt}$  for the ordering process

corral with disordered molecules  $\xrightarrow{k}$   
corral with ordered molecules

where  $F_d$  is the fraction of the corral population with disordered molecules,  $k$  is the rate constant for nucleation, and  $t$  is time. Once the molecules in a corral have ordered, they are never observed to revert to the disordered state. The rate of nucleation is essentially equal to the rate at which molecules form ordered arrays because growth occurs much more rapidly than nucleation (11). Rate constants have been calculated for pits of five different sizes from measurements of  $F_d$  versus the time after molecules are applied to the surface. Samples included both circular and noncircular corrals. We calculated  $k$  for each set of pits, correcting for the finite sampling time needed to acquire the data, which were collected in a continuous fashion (Table 1).

A representative example from the set of noncircular corrals used in this study is shown in Fig. 3. The use of noncircular pits allows greater variability in the area-to-perimeter ratio. The area-to-perimeter ratio

**Table 1.** Nucleation rate constants for molecular self-assembly.

Mean corral radius $\pm 1 \sigma$ (Å)	Collection time (hours)*	Corrals analyzed†	$k \pm 1 \sigma_k \ddagger$ (hour <sup>-1</sup> )
741 $\pm$ 60	4	262	0.036 $\pm$ 0.10
934 $\pm$ 96	1	36	0.286 $\pm$ 0.12
1184 $\pm$ 120	1	27	0.375 $\pm$ 0.17
1347 $\pm$ 159	1	19	0.447 $\pm$ 0.18
Noncircular§	1	40	0.215 $\pm$ 0.17

\*Time required to collect each data point used in the rate calculation. †Only isolated corrals were included in the analysis. Corrals containing nonrow structures or defects such as grain boundaries were not counted in the statistics. ‡The error in  $k$  was calculated according to the formula

$$\sigma_k = \left( \frac{1}{N} \sum_{i=1}^N \epsilon_i^2 \right)^{1/2}$$

where  $N$  is the number of data points taken in the  $F_d$  versus  $t$  plots, and  $\epsilon_i$  is the error between the fitted rate and point  $i$ . §Noncircular corrals had perimeters of  $(1.172 \pm 0.16) \times 10^3$  Å and areas of  $(2.633 \pm 0.35) \times 10^6$  Å<sup>2</sup>.

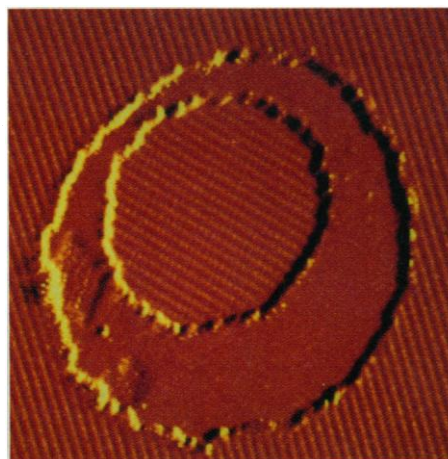


**Fig. 2.** Ordering in corrals occurs after a separate event from ordering on terraces. This figure shows two corrals, one coincidentally inside the other. Although molecules have formed an ordered monolayer in the innermost corral and on the terrace, they remain disordered in the upper corral. (Differences in the apparent resolution of features in the molecular rows inside the corral and on the terrace arise from the relative orientation of the molecular rows and the fast-scan direction of the tip. The terrace rows are more nearly perpendicular to the fast-scan direction and hence have a larger row-to-row corrugation than those in the corral.) Image size is 2000 Å by 2000 Å.

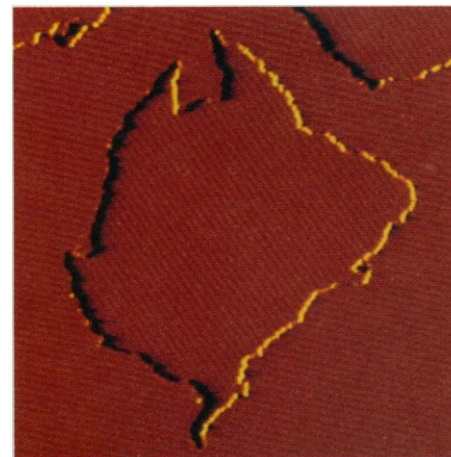


**Fig. 3.** A typical noncircular corral. The perimeter-to-area ratio for this corral is twice that of a circular corral with the same area. The use of noncircular corrals allows greater variability in the perimeter-to-area ratio than is afforded by circular corrals. The image measures 3300 Å by 3300 Å.

for these corrals is twice that of a circular corral with the same area. Despite large differences in shape, however, nucleation rates in both circular and noncircular corrals are well described by the same analysis (see below).

The length of time required for molecular ordering in corrals is strongly dependent on their size and shape; molecules in large corrals order more rapidly than molecules in small corrals. To determine the relative importance of step edge (that is, corral perimeter) versus open terrace sites (that is, corral interior) in the nucleation process, the data in Table 1 were fitted to a function with the form  $k = c_P P + c_A A$ , where  $P$  and  $A$  are the perimeter and area of the corrals, respectively, and the constants  $c_P$  and  $c_A$  reflect the relative importance of the corral perimeter and area in the nucleation process. The constants  $c_P$  and  $c_A$  are found to have the values  $(-2.7 \pm 2.5) \times 10^{-6} \text{ \AA}^{-1} \text{ hour}^{-1}$  and  $(8.6 \pm 0.6) \times 10^{-8} \text{ \AA}^{-2} \text{ hour}^{-1}$ , respectively. Figure 4 shows the nucleation rate constants for all pits plotted against the function  $c_P P + c_A A$ . A least-squares fit, calculated by weighting each point according to the inverse of its uncertainty, is shown by the dashed line.

The negative value for  $c_P$  implies that the corral perimeters, and by inference step edges, inhibit nucleation and that nucleation occurs preferentially at open terrace sites. This result is different from the nucleation behavior of most two-dimensional systems, which typically show a preference for growth initiation at substrate defects such as step edges.

The inhibitory influence of step edges and corral perimeters on film growth is also suggested by an examination of images that show molecular ordering near step edges and in highly confined regions (smaller than  $\sim 300 \text{ \AA}$  in diameter). In a typical high-resolution image of molecular ordering near a thin neck of terrace separating two corrals (Fig. 5), molecular rows in the corrals and on the terrace can be clearly resolved away from the corral edges but lose

definition close to the edges ["frizziness" (12)]. The molecular rows on the terrace do not extend into the highly confined, narrow terrace isthmus between the corrals, and, in this case, a small group of molecules has ordered into a nonrow structure in that area. Close inspection of Fig. 1A shows the same lack of order on the terrace between the corrals that almost touch. Although these results are typical of the behavior of films of this molecule in highly confined regions and at step edges, in a minority of cases molecular rows are observed to extend directly to corral edges, both inside of corrals and on the surrounding terrace. The overall trend, however, suggests that ordering does not occur as readily in highly confined regions or near step edges or corral perimeters as it does away from them. These observations are consistent with the negative sign of  $c_P$ .

The arrangement of molecules in a self-assembled film reflects a balance of molecule-molecule and molecule-substrate interactions that results in a minimum free-energy configuration. At step edges and other defects, the nature of the molecule-substrate interaction may change, disturbing the balance and favoring the formation of a different molecular arrangement. For films of this molecule under the present conditions, the preferred molecular arrangement at step edges and in highly confined regions is a more disordered one. Molecular disorder at step edges may be used to explain the effect step edges exert on nucleation rates. Nucleation during self-assembly is thought to begin with the formation of small ordered clusters of molecules generated by thermal fluctuations. These clusters must attain a critical size before the addition of new molecules (that is, growth) becomes favored. If nucleation occurs near a step, the tendency of steps to promote molecular disorder may make it more difficult for the cluster to attain its critical size. This effect leads to a decreased rate of successful nucleation and molecular self-assembly near corral edges and mani-

fest itself as the negative coefficient of the perimeter term in the fitted form of the rate expression.

If nucleation occurs away from corral edges as the above analysis suggests, then the ordering of molecules in corrals should bear only a weak relation to the ordering of molecules on the terrace, if any. Two convenient probes of this relation are the relative directional alignment of the molecular rows inside the corrals with those on the terrace and the relative chirality, or "helicity," of the molecular rows (13). Constrained to two dimensions, 8CB is chiral and forms left-handed and right-handed structures with equal probability. The ratio of the number of corrals containing molecules organized with the same chirality as those on the terrace reflects the degree of independence of nucleation in corrals, with a ratio of 50:50 expected for complete independence and a ratio of 100:0 expected for strongly coupled nucleation. The ratio measured from the corrals in the present study was 58:42 with a marginal error of 3% and was independent of corral size, indicating that the chirality of molecular rows in corrals is only weakly influenced by molecules on the nearby terrace.

Conversely, a second measure, the relative directional alignment of molecular

**Fig. 4.** Dependence of the nucleation rate constant on corral size and shape. The dashed line is a weighted fit to determine the relative importance of corral perimeter and area on nucleation rate. Ordinate errors are listed in Table 1. Abscissa errors are calculated from a propagation-of-error analysis based on the standard deviations of the measured corral perimeters and areas.

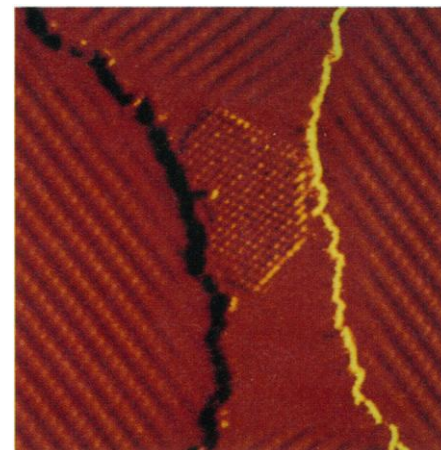
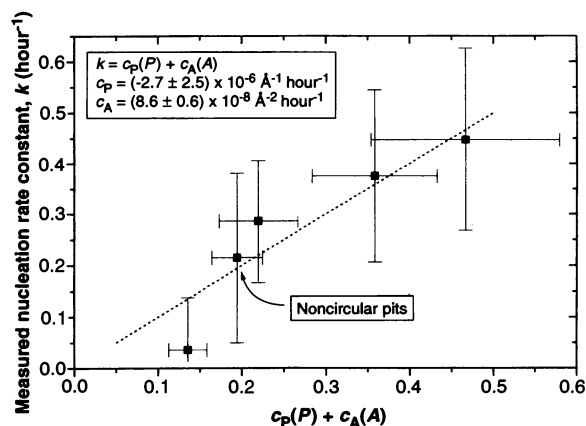


**Fig. 5.** Effect of step edges, corral perimeters, and highly confined regions on molecular ordering. The image shows an 1100  $\text{\AA}$  by 1100  $\text{\AA}$  constant-height STM image of an ordered 8CB film near a thin isthmus of terrace separating two corrals. Note the absence of molecular rows near corral perimeters and on the spatially confined isthmus between the corrals. In this case, a small patch of molecules arranged in a different configuration is occupying a portion of the space between the corrals. This configuration is seen only in highly confined spaces or against step edges and is molecular in origin (that is, not a graphite flake) because the positions of the image features are fluxional with time. The molecules may be 8CB or molecular impurities.

rows, exhibits a stronger correlation between molecules in corrals and molecules on terraces. When the molecular rows in a corral have the same chirality as the rows on the nearby terrace, they can either align in the same direction or form intersection angles of  $\pm 120^\circ$ . The threefold symmetry of graphite prohibits any other angles (14). Measurements of the intersection angle reveal a strong tendency for molecular rows in corrals to align in the same direction as those on the terrace. Intersection angles of  $\pm 120^\circ$  are observed in less than 20% of all corrals studied. In the absence of orientational interactions, the expected purely statistical value would be 67%. Also in contrast to the case for the chirality ratio, the tendency of molecular rows in corrals to align in the same direction as those on the terrace depends strongly on corral size. In small corrals ( $\sim 500$  Å in radius), the proportion aligned at  $\pm 120^\circ$  approaches 0% but increases steadily to 18% for corrals 1347 Å in radius, the largest size studied. This trend appears to reflect an unexpectedly long-range orientational interaction, acting over tens or hundreds of angstroms. It may perhaps be communicated through second and higher layers of 8CB not adsorbed directly to the substrate (15).

These findings demonstrate that molecule corrals permit the analysis of a large number of semi-independent, nanometer-sized sample ensembles, each with an identical thermal history. A statistical approach can be taken to STM data analysis that may open new avenues for observing and modeling surface phenomena by scanning probe microscopy. Corrals may also be used in studies of confinement effects on monolayer structure, in the determination of activation energies for nucleation through variable-temperature STM, in studies of the strength and distance dependence of molecular interactions between nearby crystalline domains, and in the calculation of the relative configurational free energies of different molecular structures from their measured occurrence probabilities.

## REFERENCES AND NOTES

1. A. Ulman, *An Introduction to Ultrathin Organic Films* (Academic Press, San Diego, CA, 1991).
2. G. M. Whitesides, J. P. Mathias, C. T. Seto, *Science* **254**, 1312 (1991).
3. M. F. Crommie, C. P. Lutz, D. M. Eigler, *ibid.* **262**, 218 (1993).
4. H. Chang and A. J. Bard, *J. Am. Chem. Soc.* **112**, 4598 (1990).
5. ———, *ibid.* **113**, 5588 (1991).
6. X. Chu and L. D. Schmidt, *Carbon* **29**, 1251 (1991); *Surf. Sci.* **268**, 325 (1992); F. Atamny, R. Schlogl, W. J. Wirth, J. Stephan, *Ultramicroscopy* **42**, 660 (1992); L. M. Siperko, *J. Vac. Sci. Technol. B* **9**, 1061 (1991).
7. J. S. Foster and J. E. Frommer, *Nature* **333**, 542 (1988).
8. D. L. Patrick and T. P. Beebe Jr., *Langmuir* **10**, 298 (1994), and references therein.
9. R. Hentschke, B. L. Schürmann, J. P. Rabe, *J. Chem. Phys.* **96**, 6213 (1992).

10. The effect of tip-induced ordering and nucleation was considered and rejected, because the rate constants did not depend on the amount of time the sample was scanned.
11. For those rare times in which molecules in a corral order during imaging, the process is completed within the time required to collect a few points along a scan line (tens of milliseconds). Furthermore, partially ordered corrals are never observed: Corrals are either completely ordered or disordered.
12. L. Kuipers, M. S. Hoogeman, J. W. Frenken, *Phys. Rev. Lett.* **71**, 3517 (1993).
13. The helicity (handedness) of an 8CB monolayer describes whether the periodic dislocation that occurs every fourth molecule is toward the left or toward the right when viewed along a row (see Fig. 1B). Domains with opposite helicities are mirror images of one another, not superimposable by rotation alone [see D. P. E. Smith, *J. Vac. Sci. Technol. B* **9**, 1119 (1991)].
14. When the chirality of molecular rows is different,

other intersection angles are possible. For simplicity, we discuss here only the subset of pits containing molecular rows with the same chirality as the terrace; however, pits with molecular rows of different chirality than the terrace follow a similar trend.

15. At the temperatures used in this study, bulk 8CB is a layered smectic-A phase with an interlayer distance similar to the interrow spacing of the molecules adsorbed to graphite (29 to 32 Å versus  $\sim 38$  Å) (7). If the smectic planes are oriented approximately normal to the surface in the region of the substrate, they could provide an efficient route for promoting long-range alignment.
16. We thank C. Wight and P. Armentrout for suggestions. Supported by the NSF (National Young Investigator Award CHE-9357188). T.P.B. is a Camille Dreyfus Teacher-Scholar. V.J.C. is a Herbert I. and Elsa B. Michael Fellow.

1 April 1994; accepted 25 May 1994

## Peptide Synthesis Catalyzed by an Antibody Containing a Binding Site for Variable Amino Acids

Ralph Hirschmann,\* Amos B. Smith III,\* Carol M. Taylor, Patricia A. Benkovic, Scott D. Taylor, Kraig M. Yager, Paul A. Sprengeler, Stephen J. Benkovic\*

Monoclonal antibodies, induced with a phosphonate diester hapten, catalyzed the coupling of *p*-nitrophenyl esters of *N*-acetyl valine, leucine, and phenylalanine with tryptophan amide to form the corresponding dipeptides. All possible stereoisomeric combinations of the ester and amide substrates were coupled at comparable rates. The antibodies did not catalyze the hydrolysis of the dipeptide product nor hydrolysis or racemization of the activated esters. The yields of the dipeptides ranged from 44 to 94 percent. The antibodies were capable of multiple turnovers at rates that exceeded the rate of spontaneous ester hydrolysis. This achievement suggests routes toward creating a small number of antibody catalysts for polypeptide syntheses.

The chemical synthesis of large peptides has been accomplished by two distinct but not mutually exclusive approaches. The first, involving the stepwise addition of single amino acids from the COOH- to the NH<sub>2</sub>-terminus (1), was revolutionized by the advent of the Merrifield solid-phase technique (2), in combination with reversed-phase, high-performance liquid chromatography (HPLC) purification techniques (3, 4). Fragment condensation, the second approach, permitted the first total synthesis of an enzyme in solution in 1969 (5). The fragment condensation strategy is particularly attractive for the synthesis of chemically related proteins that differ in

one or more of the fragments. Solubility problems, a result of multiple hydrophobic protecting groups, have limited the usefulness of this approach. In an effort to overcome this problem, proteolytic enzymes have been used in peptide bond formation (6). This variation of the fragment condensation method is also beset by limitations, principally product inhibition and the susceptibility of the products to cleavage at positions corresponding to the natural hydrolytic sites.

The advent of antibodies as catalysts (7) for organic transformations suggested another approach to the coupling of unprotected amino acids and peptide fragments that potentially would exceed the scope and specificity attainable with proteolytic enzymes as catalysts. We report here the antibody-catalyzed formation of a dipeptide (8).

The traditional approach to generating catalytic antibodies involves the design of haptens that are topologically and structurally nearly identical to the transition state of the reaction. For peptide synthesis (Fig. 1), this strategy has two shortcomings: first, a large

R. Hirschmann, C. M. Taylor, K. M. Yager, P. A. Sprengeler, Department of Chemistry, University of Pennsylvania, Philadelphia, PA 19104, USA.  
A. B. Smith III, Department of Chemistry, Laboratory for Research on the Structure of Matter, Monell Chemical Senses Center, University of Pennsylvania, Philadelphia, PA 19104, USA.  
P. A. Benkovic, S. D. Taylor, S. J. Benkovic, Department of Chemistry, Pennsylvania State University, University Park, PA 16802, USA.

\*To whom correspondence should be addressed.